

**Abstract.** The lithium abundances in metal-poor halo stars are of importance for cosmology, galaxy evolution and stellar structure. In an attempt to study possible systematic errors in the derived Li abundances, the line formation of Li I lines has been investigated by means of realistic 3D hydrodynamical model atmospheres of halo stars and 3D non-LTE radiative transfer calculations. These are the first detailed 3D non-LTE computations reported employing a multi-level atomic model showing that such problems are now computationally tractable. The detailed computations reveal that the Li I population has a strong influence from the radiation field rather than the local gas temperature, indicating that the low derived Li abundances found by Asplund et al. (1999) are an artifact of their assumption of LTE. Relative to 3D LTE, the detailed calculations show pronounced over-ionization. In terms of abundances the 3D non-LTE values are within 0.05 dex of the 1D non-LTE results for the particular cases of HD 140283 and HD 84937, which is a consequence of the dominance of the radiation in determining the population density of Li I. Although 3D non-LTE can be expected to give results rather close ( $\approx \pm 0.1$  dex) to 1D non-LTE for this reason, there may be systematic trends with metallicity and effective temperature.

**Key words:** Line: formation – Radiative transfer – Stars: abundances – Stars: atmospheres – Stars: Population II

# Multi-level 3D non-LTE computations of lithium lines in the metal-poor halo stars HD140283 and HD84937

Martin Asplund<sup>1</sup>, Mats Carlsson<sup>2</sup>, and Andreas V. Botnen<sup>2</sup>

<sup>1</sup> Research School of Astronomy, Mt. Stromlo Observatory, Cotter Road, Weston, ACT 2611, Australia

<sup>2</sup> Institute of Theoretical Astrophysics, University of Oslo, P.O. Box 1029, Blindern, N-0315 Oslo, Norway

## 1. Introduction

Lithium abundances of metal-poor halo stars have had a prominent place in astrophysics and cosmology ever since the first discovery of Li in such stars (Spite & Spite 1982) due to their wide-ranging implications. Firstly, the uniformity of the Li abundances in halo stars (Ryan et al. 1999) presumably reflects the primordial Li abundance stemming from Big Bang nucleosynthesis, thus allowing an estimate of the baryon density of the Universe. Secondly, any observed slope in the Spite-plateau with metallicity, when combined with the corresponding behaviour of <sup>6</sup>Li, Be, B and O, can be interpreted in terms of Galactic chemical evolution, in particular the history of cosmic ray spallation in the early Galaxy. Thirdly, since it is a fragile element, Li can function as a tracer of stellar mixing; the thinness of the Spite-plateau certainly severely limits the allowed amount of Li-depletion in halo stars (Ryan et al. 1999).

In order to extract Li abundances from an observed spectrum it is necessary to have suitable models of the stellar photosphere and the line formation process. Since traditional abundance analyses utilize 1D hydrostatic model atmospheres based on local thermodynamic equilibrium (LTE) and a rudimentary description of convection in the form of the mixing length theory (MLT), there may be significant systematic errors, which could distort the derived conclusions. The detailed line formation, including departures from LTE but in 1D hydrostatic model atmospheres, were investigated by Carlsson et al. (1994) who found relatively small non-LTE abundance corrections ( $\lesssim 0.05$  dex) for low metallicity stars. To investigate the effects of convection on the line formation, Asplund et al. (1999) applied the new generation of 3D, hydrodynamical model atmospheres to abundance analyses of metal-poor stars assuming LTE. Due to the much lower temperatures encountered in the line-forming layers than in classical 1D model atmospheres, the derived abundances differ drastically. Most notably, it was found that the primordial Li abundance may previously have been over-estimated by  $\simeq 0.3$  dex. Although such 3D model atmospheres should

be a more realistic description of the stellar photospheres (Asplund et al. 2000), the simplification of LTE in the line formation is a crucial assumption. Asplund et al. (1999) indeed warned that the steep temperature gradients may be prone to significant over-ionization of species like Li I. The aim of the present paper is to investigate possible departures from LTE by performing realistic 3D non-LTE calculations for Li I lines, while we defer a detailed investigation of the line formation to a subsequent article. Preliminary calculations have been presented in Asplund (2000) using a smaller Li atom and without consideration of line-blanketing.

## 2. 3D non-LTE radiative transfer of Li I lines

From the *ab-initio* 3D radiative-hydrodynamical convection simulations of the metal-poor halo stars HD 140283 and HD 84937 presented in Asplund et al. (1999), two representative and independent snapshots have been selected from each simulation for the non-LTE calculations. Additionally, two snapshots were taken from a similar solar simulation (Asplund et al. 2000a) for comparison purposes. The original simulation data cubes with dimensions  $100^2 \times 82$ , were interpolated prior to the non-LTE calculations to a  $25^2 \times 100$  grid with an improved vertical resolution. Test calculations with  $50^2 \times 100$  snapshots verified that the procedure had insignificant effect on the 3D non-LTE abundance corrections. Typically the atmospheric structures cover the region  $-6 \leq \log \tau_{500} \leq 2$ . Further details of the numerical simulations are available in Stein & Nordlund (1998) and Asplund et al. (1999, 2000).

The Li model atom employed in the present study is identical to the one compiled by Carlsson et al. (1994). The adopted 21-level atom consists of in total 70 bound-bound and 20 bound-free radiative transitions. We feel confident that the employed Li atom is sufficiently extended as tests with a more restricted 12-level atom revealed non-LTE abundance corrections only about 0.03 dex larger than with the 21-level atom for HD 140283 and HD 84937. The input data for level energies, radiative and electron collisional transitions are in all cases the same as in Carlsson et al. (1994); accordingly, collisions with

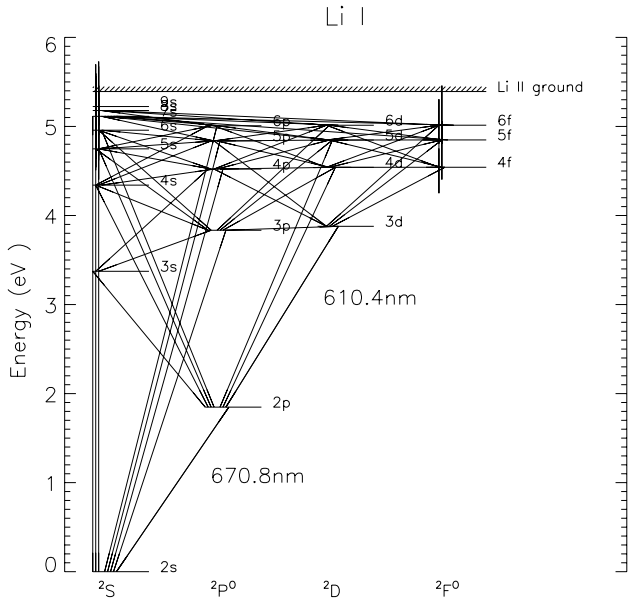


**Fig. 1.** Grotrian termdiagram for the adopted 21-level Li model atom. All levels are connected with the Li II ground state by photo-ionization transitions.

**Table 1.** Predicted LTE and non-LTE flux equivalent widths (in pm=10 mÅ) of the Li I 670.8 nm line for the Sun, HD 140283 and HD 84937 in 1D and 3D. The 3D equivalent widths are the average of two independent snapshots.

Star	$\log \epsilon_{\text{Li}}$	1D		3D	
		$W_{\lambda}^{\text{LTE}}$	$W_{\lambda}^{\text{NLTE}}$	$W_{\lambda}^{\text{LTE}}$	$W_{\lambda}^{\text{NLTE}}$
Sun	1.1	0.40	0.34	0.55	0.37
HD 140283	1.8	2.38	2.18	3.84	1.96
	2.2	4.90	4.76	7.67	4.21
HD 84937	2.0	1.31	1.44	1.79	1.11
	2.4	2.91	3.29	4.00	2.55

neutral hydrogen have not been included. We have verified that even inclusion of H collisions according to the classical Drawin (1968) recipe has a very minor impact on our results: for HD 140283 the abundance corrections are decreased by 0.05 dex and 0.01 dex for multiplication factors of 1.0 and 0.01, respectively, of the standard Drawin estimates. Additional atomic data such as background opacities (including line-blanketing for photo-ionization transitions) are taken from the MARCS package (Gustafsson et al. 1975 and subsequent updates).

The non-LTE calculations for Li have been performed with MULTI3D (Botnen 1997; Botnen & Carlsson 1999), which is essentially a 3D-version of the widely used MULTI-code for 1D statistical equilibrium problems (Carlsson 1986). MULTI3D iteratively solves the rate equations with a consistent radiation field obtained from a simultaneous solution of the radiative transfer equation along 24-48 in-

clined rays. The formal solution of the radiative transfer equation is computed using a short characteristic technique, making use of the horizontal periodic boundary conditions of the hydrodynamical model atmospheres. The Doppler shifts introduced by the convective motions are taken into account and therefore no micro- and macro-turbulence enter the analysis (Asplund et al. 2000). Typically  $\lesssim 6$  accelerated lambda-iterations with linearization and preconditioning of the rate equations (Scharmer & Carlsson 1985) were necessary to achieve the stipulated convergence criteria  $\max(\delta n_i/n_i) < 10^{-4}$ . The resulting angle-dependent radiation field was subsequently used to compute flux profiles. Various test calculations with 3D-extended plane-parallel homogeneous model atmospheres ensured that the same results were obtained with MULTI3D and MULTI.

### 3. Departures from LTE in Li I line formation

Table 1 summarizes the resulting 3D LTE and non-LTE line strengths for the different snapshots and input Li abundances together with the corresponding 1D results. Clearly, there are very significant departures from LTE, in particular for the two metal-poor stars. As predicted by Asplund et al. (1999), over-ionization plays the dominant role.

Fig. 2 shows images of the continuum intensity and the equivalent width of the Li I 670.8 nm line in LTE and non-LTE at disk-center ( $\mu = 1.0$ ). The characteristic granulation pattern with warm (bright) upflows and cool (dark) downflows is clearly visible in the continuum intensities. In LTE the Li line typically is strong above the granules, a consequence of the low temperatures in the optically thin layers due to the temperature contrast reversal in the convectively stable layers, which translates to a high population density of Li I. Over the downflows the temperatures tend to be higher than average, thus making the Li line weaker. In non-LTE quite the opposite happens: in general the line is weaker above the upflows, which implies that the population density is largely controlled by the radiation field rather than the local gas temperature.

The same conclusion is obvious from Fig. 3, which quantifies the behaviour in Fig. 2. The Li I lines tend to increase in strength with continuum intensity in LTE but with a very large scatter, since the temperatures in the higher atmospheric layers are not one-to-one correlated with the temperatures in the continuum-forming layers below. In non-LTE the scatter is much smaller for regions with high continuum intensities, which again emphasizes that the line formation process is largely governed by the non-local properties of the radiation field. The 670.8 nm line is, however, weakest in relatively low continuum intensity regions ( $I^{\text{cont}}/\langle I^{\text{cont}} \rangle \simeq 0.9$  in Fig. 3) which are immediately adjacent to very bright regions: the non-vertical hot radiation field from neighboring granules cause significant over-ionization (low line opacity) which when coupled

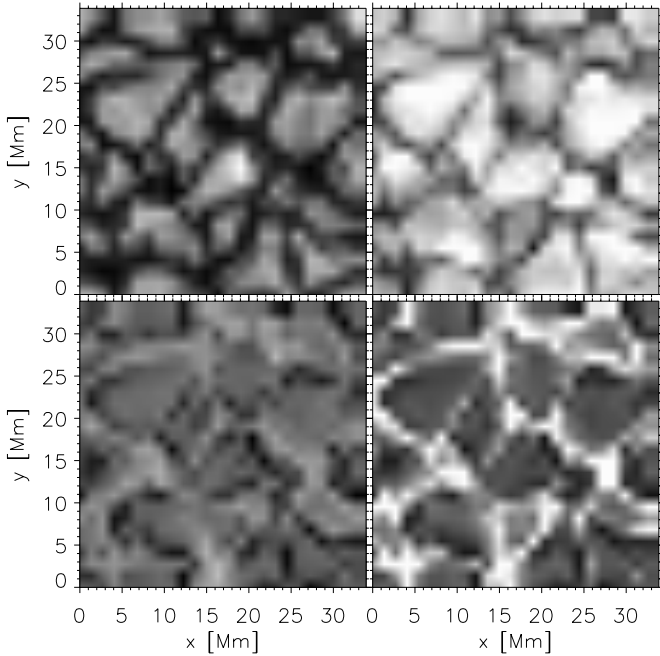


**Fig. 2.** Granulation pattern in snapshot 1 of HD 140283 seen in disk-center continuum intensity (*upper left panel*) and equivalent width of the Li I 670.8 nm line in LTE (*upper right panel*) and non-LTE (*lower left panel*); the equivalent width images have the same relative intensity scale to emphasize the overall difference in line strengths. Also shown is the ratio of the non-LTE and LTE equivalent widths (*lower right panel*).

to the shallow temperature gradient of downflows makes the line very weak (e.g. at  $x = 21$  Mm and  $y = 18$  Mm in Fig. 2). The Li I line typically is strongest in the middle of larger areas of downflowing material, which has weaker photo-ionizing radiation field (e.g. at  $x = 9$  Mm and  $y = 13$  Mm). The non-LTE behaviour of the Li I 670.8 nm line shown in Figs. 2 and 3 is similar to the findings of Kiselman (1997, 1998) and Uitenbroek (1998) in the case of the Sun, which are confirmed by spatially resolved solar observations (Kiselman & Asplund 2001). The Li I 610.4 nm line show a similar behaviour as the resonance line although less dramatically due to the weakness of the line and its higher excitation potential (Fig. 3).

Further support for the departures from LTE being essentially an over-ionization effect comes from the variation with height of the departure coefficient of the Li I ground level (Fig. 4). From the LTE-expectation in the deeper layers, the population density falls rapidly with height as Li I is photo-ionized by radiation from below. The non-LTE line formation of the Li I 670.8 nm line is mainly an optical depth effect since the line source function  $S_\nu^{670.8}$  in general remains reasonably close to the Planck function  $B_\nu(T)$  (Fig. 4). As in the 1D case, the over-ionization is predominantly driven by photo-ionization from the 2p state for which  $J_\nu/B_\nu$  is near its maximum (Carlsson et al. 1994). The inclusion of line opacities to the back-

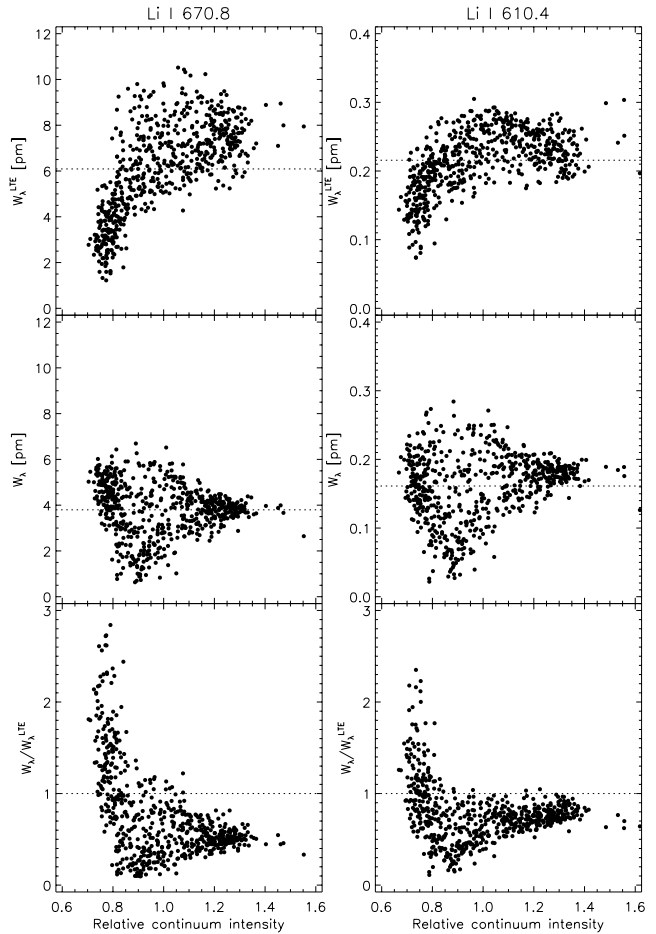


**Fig. 3.** Predicted intensity ( $\mu = 1.0$ ) equivalent widths of the Li I 670.8 nm (*left panel*) and 610.4 nm (*right panel*) lines across the granulation pattern in LTE (*upper panel*) and non-LTE (*middle panel*) for the HD 140283 simulation with  $\log \epsilon_{\text{Li}} = 2.20$ . The mean intensity equivalent widths are denoted by horizontal lines. Also shown are the ratios of non-LTE and LTE equivalent widths (*lower panel*).

ground opacities for bound-free transitions is thus of importance: without line-blanketing the non-LTE abundance corrections for HD 140283 would be about 0.07 dex higher. As expected the radiative rates dominate over the corresponding collisional rates for the 2s and 2p levels.

The speculation by Kurucz (1995) that the strength of the Li I 670.8 nm line could be seriously overestimated with 1D models due to substantial departures from LTE in the presence of temperature inhomogeneities, is thus partly validated by our results, although for the wrong reasons and to a much lesser extent. Due to his simple two-stream MLT-convection approach, Kurucz also failed to recognize the compensating effect due to convection (Asplund et al. 1999; Asplund 2000). Cayrel & Steffen (2000) reached similar conclusions to ours based on calculations using a 5-level Li atom and a 2D simulation of a metal-poor Sun.

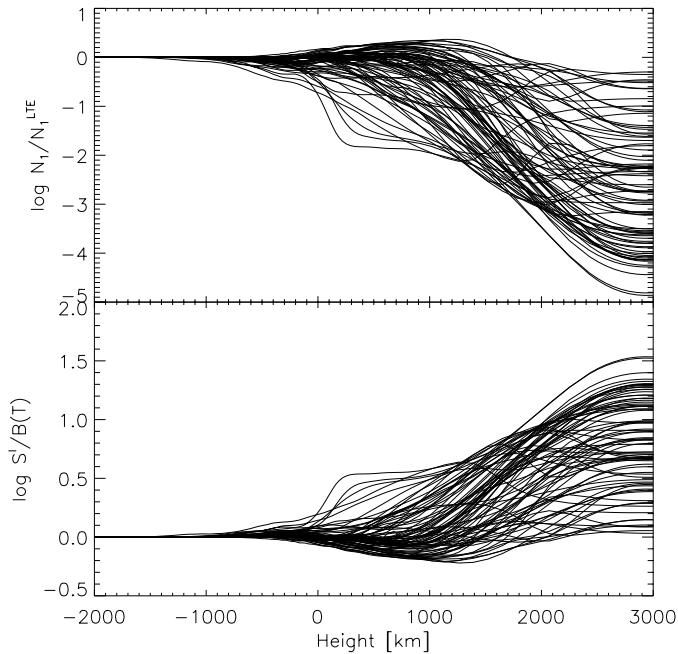


**Fig. 4.** Variation of the departure coefficient of the Li I ground level  $N_1/N_1^{\text{LTE}}$  (*upper panel*) and  $S_\nu^{670.8}/B_\nu(T)$  (*lower panel*) as a function of atmospheric height for the HD 140283 simulation. Selected vertical columns are connected with solid lines.

#### 4. Discussion

With the aid of Table 1, it is possible to interpolate the computed 1D and 3D line strengths to the observed equivalent widths of Li I 670.8 nm for HD 140283 (4.65 pm) and HD 84937 (2.44 pm). It is noteworthy that the 3D non-LTE abundances only differ by  $\lesssim 0.05$  dex from the corresponding 1D non-LTE results for HD 140283 and HD 84937. The 3D LTE abundances on the other hand are distinctly different by 0.2 – 0.3 dex. As cautioned by Asplund et al. (1999), LTE is clearly a very poor assumption for Li I in 3D models of halo stars with their low surface temperatures and steep temperature gradients<sup>1</sup>.

The 3D non-LTE abundances are very similar to the 1D non-LTE results. The main reason for this is that the line strength is determined by the opacity which is set by the photoionizing radiation field while collisions are found to be relatively unimportant according to our calculations<sup>2</sup>. This radiation is optically thin at the height of formation of the Li I resonance line and is thus equal to the observable emergent radiation field. Since 1D and 3D models produce similar ( $\pm 10\%$ ) emergent intensities at the relevant wavelengths (Asplund & García Pérez 2001),

<sup>1</sup> This statement is of course not true in general, as LTE may be a very good approximation for other species.

<sup>2</sup> We note that the approximate ionization equation (e.g. Mihalas 1978, Eq. 5.46) is not applicable as a possible explanation for the similarity of the 1D and 3D results, since the downward rate from Li II is dominated by collisions to upper levels rather than by photo-recombination to the ground level.

the photo-ionization radiation fields will not differ significantly. The final line strengths will however also depend on the details of the temperature structures in the deep atmospheric layers which differs between 1D and 3D models.

From the results obtained here for two typical halo stars we expect that the 3D non-LTE abundances will be similar ( $\approx \pm 0.1$  dex) to the 1D non-LTE results (and to 1D LTE given the small 1D non-LTE abundance corrections according to Carlsson et al. 1994) in general for halo stars. However, given the great interest in accurately determining the primordial Li abundance, the intrinsic scatter in the Spite-plateau and the possible existence of a trend with metallicity for the Li abundances (e.g. Ryan et al. 1999), it is clearly important to extend the 3D non-LTE calculations to additional stars with different parameters to determine exactly the net 3D effects. We are currently working towards this goal (Asplund et al., in preparation).

*Acknowledgements.* It is a pleasure to thank R. Cayrel, R. Collet, A.E. García Pérez and D. Kiselman for stimulating discussions and the referees for helpful comments. This work has been supported by grants from the Swedish and Norwegian Research Councils.

#### References

- Asplund, M. 2000, in IAU Symp. 198, The light elements and their evolution, ed. L. Da Silva et al., 448
- Asplund, M., & García Pérez, A.E. 2001, A&A, 372, 601
- Asplund, M., Nordlund, Å., Trampedach, R., & Stein, R.F., 1999, A&A, 346, L17
- Asplund, M., Nordlund, Å., Trampedach, R., Allende Prieto, C., & Stein, R.F. 2000, A&A, 359, 729
- Botnen, A.V. 1997, Cand. Sci. Thesis, University of Oslo
- Botnen, A.V., & Carlsson, M. 1999, in Numerical astrophysics, ed. S.M. Miyama et al., 379
- Carlsson, M. 1986, Uppsala Astronomical Report No. 33
- Carlsson, M., Rutten, R.J., Bruls, J.H.M.J., & Shchukina, N.G. 1994, A&A, 288, 860
- Cayrel, R., Steffen, M. 2000, in IAU Symp. 198, The light elements and their evolution, ed. L. Da Silva et al., 437
- Drawin, H.W. 1968, Z. Phys., 211, 404
- Gustafsson, B., Bell, R.A., Eriksson, K., & Nordlund, Å. 1975, ApJ, 42, 407
- Kiselman, D. 1998, A&A, 333, 732
- Kiselman, D. 1997, ApJ, 489, L107
- Kiselman, D., & Asplund M. 2001, in ASP Conf. Ser. 223, Cool stars, stellar systems and the Sun, ed. R.J. García López et al., 684
- Kurucz, R.L. 1995, ApJ, 452, 102
- Mihalas D., 1978, Stellar atmospheres, W.H. Freeman and Company, San Francisco
- Ryan, S.G., Norris, J.E., & Beers, T.C. 1999, ApJ, 523, 65
- Scharmer, G.B., & Carlsson, M. 1985, J. Comp. Phys., 59, 56
- Spite, F., & Spite, M. 1982, A&A, 115, 357
- Stein, R.F., & Nordlund, Å. 1998, ApJ, 499, 914
- Uitenbroek, H. 1998, ApJ, 498, 427